

# RECONSTRUCTION 1989- 2005 INUNDATION HISTORY IN THE OKAVANGO DELTA FROM ARCHIVAL LANDSAT TM IMAGERY

Piotr Wolski<sup>(1)</sup>, Michael Murray-Hudson<sup>(1)</sup>

<sup>(1)</sup> Harry Oppenheimer Okavango Research Centre, Private Bag 285, Maun, Botswana, Email: [pwolski@orc.ub.bw](mailto:pwolski@orc.ub.bw)

## ABSTRACT

Reconstruction of the inundation history in the flood-pulsed 12000 km<sup>2</sup> wetland of the Okavango Delta is a prerequisite for the calibration of hydrological models, development of ecological models, and improved understanding of geomorphological dynamics of this system. Although flood mapping has been previously done based on NOAA AVHRR data, there is a need for higher resolution inundation maps. Fourteen Landsat TM5 and TM+ coverages (4 scenes each), depicting the largest annual inundation extent for the periods 1989-1990, 1992-2002 and 2005 are analysed in this study. Initial analyses indicated that separability of “dry” and “inundated” Landsat TM spectral signatures is affected by the presence of extensive floating *Cyperus papyrus* mats that entirely cover underlying water, and the presence of evergreen riverine forests. These render inapplicable such classic methods of land/water discrimination as thresholding of Tasseled Cap wetness product and the thermal band. Additionally, the dynamics of the system prohibit ground-truthing of classification results of historic imagery. To overcome these difficulties, a classification procedure has been devised that is based on a combination of supervised and unsupervised classification of multispectral data and indices (band 5 and 2 ratio), and contextual analyses.

## 1. INTRODUCTION

Mapping of inundation in wetlands is one of the primary applications of passive remote sensing (RS) in wetland science and hydrology. Current attention, however, focuses on the use of Synthetic Aperture Radar (SAR) imagery, which is understandable, as this active microwave technique has capacity to overcome the main disadvantage of optical sensors, i.e. the inability to “sense” under cloud and vegetation cover. However, operationally usable radar images are available only since ca. 2000, while passive RS images are available from as far back as the 1970s, which makes them very useful in longer-term ecological studies e.g. [1].

The Okavango Delta (OD) is a flood-pulsed wetland located in dry northern Botswana. Inundation extent in this system varies between 3500 km<sup>2</sup> and 12000 km<sup>2</sup> on a seasonal and inter-annual basis, and this variation is a principal driver of a diverse and unique ecosystem. The OD is the largest Ramsar site in the world, is the basis

for subsistence of the local population and the core of Botswana’s tourism industry, which is the country’s second largest source of revenue.

Recently, a reconstruction of the inundation history in the OD was done using NOAA AVHRR images [2]. The classification procedure was based on unsupervised classification. Other studies focused on derivation of snapshot land-cover [3] and vegetation [4] maps from Landsat images. In the former, land/water discrimination was obtained by thresholding of Tasseled Cap (TC) wetness and the TM5/TM2 band ratio, with regionally varying threshold values. In the latter, unsupervised classification was used. Time series inundation maps of a part of the system was obtained also in the context of studying the occurrence and ecological effects of fire [5]. In that study, the land/water discrimination procedure was based on unsupervised classification of La. SAR images have also been used in the Okavango Delta [6,7].

The emergent need in the OD is the quantification of the hydroperiod-vegetation relationship and biodiversity studies, in which knowledge of flooding history at the plot scale is the principal prerequisite. Additionally, assessment of the causes of observed changes in the hydrological system (flood shifts) is contingent on detailed inundation maps.

The study reported here was aimed at derivation of inundation maps covering the period 1989-2005. This was done in the framework of a paucity of data to assist in the classification of historic RS images, and thus an accurate and robust method that demands little subjectivity was sought after. In this paper, we firstly describe the characteristics of inundation in the OD, in the context of the inundation-vegetation-spectral response relationship. We then test several commonly used methods of land/water discrimination. Subsequently, we present an adopted method of classification and final results of the classification.

## 2. MATERIALS AND METHODS

Work presented here is based on fourteen Landsat (TM 5 and TM+) coverages of the Okavango Delta, each containing 4 scenes (WRS 175/74, 175/73, 174/74 and 174/73). The coverages were obtained for 1989-2005,

with the exception of 1991, 2003 and 2004, for which images were not available. For each year, the dates of images were selected to represent as closely as possible the maximum annual inundation extent in the Okavango Delta, which usually occurs between in August or September. Each of the images was georeferenced by image-to-image registration to the rectified (UTM WGS 84 coordinate system) Landsat images available from Global Land Cover Facility ([www.glcapp.umiacs.uml.edu](http://www.glcapp.umiacs.uml.edu)). In land/water classification, TM bands 1-7 (6a in case of TM+) were used. For the purpose of classification, products such as the standardized ratio of TM band 5 to TM band 2, and Tasseled Cap (TC) wetness component were derived. All image processing and classification was done using ERDAS IMAGINE 8.4.

Aerial photomosaics of July-August 2002 survey were obtained from the Botswana Department of Surveys and Mapping. The photomosaics were in digital format at 1 m resolution, in the UTM WGS 84 coordinate system.

To assess the various methods of land/water discrimination, a single Landsat TM image (WRS 174/73) from 28 August 2002 (corresponding to the date of the aerial photomosaic) was used. Inundation status was determined from aerial photomosaics for a set of 256 points distributed randomly within the scene. The status of these points was compared to inundation status determined by each of the methods tested. The Kappa coefficient and the total percentage accuracy were used as indices of classification accuracy. The following methods of land/water discrimination were assessed: a) thresholding of TM6, b) thresholding of TM5/TM2 ratio, c) thresholding of TC3 (wetness) component, d) unsupervised classification (ISODATA) into 20 classes with subsequent allocation of classes into inundated/dry, and e) supervised classification (using maximum likelihood, minimum distance and Mahalanobis distance classifiers).

The final procedure for land/water discrimination was developed based on the analysis of spectral characteristics of various inundation-vegetation classes. The final method was verified by applying it to a different scene (WRS 174/74) from the same period, and using a second set of 256 randomly distributed points, the inundation status of which was determined from the aerial photomosaic.

The method was consequently applied to each Landsat scene available in the study; and the "scene" inundation maps were then merged (datewise) to produce inundation maps for the entire system. These were subsequently used to produce an annual inundation frequency map.

### 3. INUNDATION AND SPECTRAL RESPONSES IN THE OKAVANGO DELTA

Flooding in the OD is very dynamic, and the extent of inundation varies on both an annual and inter-annual basis. The vegetation (density and species composition) of inundated areas changes depending on the recent (months) and longer-term (years) inundation history. As yet, these changes have not been quantitatively described, and our study is, in fact, the first step towards such a description. However, the results of earlier studies (summarized in e.g. [8]) and knowledge of the area allows for the following generalization of the inundation-vegetation-morphology settings.

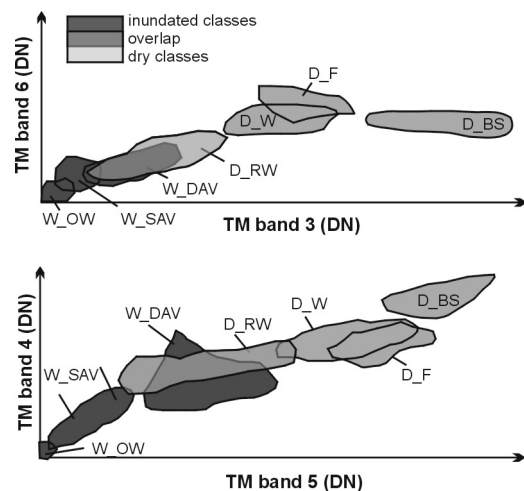


Figure 1 Reflectance envelopes of inundation-vegetation classes

There is a distinct difference in vegetation between "floodable" and "non-floodable" areas, resulting from the tree species occurring in the OD being intolerant to inundation [8]. Topographically higher land and land that has not been inundated for many years (>30) is thus usually covered by trees. Topographically lower land that is subject to even occasional inundation, is covered by grasses and herbs (when dry) or various aquatic vegetation communities (when inundated). The permanently inundated areas are covered by obligatory aquatic species. The following typical vegetation-inundation classes can be distinguished:

- deep open water of lagoons and channels (W\_OW)
- dense aquatic vegetation comprising a floating mat of *Cyperus papyrus* and rooted large emergents (*Miscanthus*, *Phragmites spp*) or other obligatory aquatic plants (W\_DAV) in permanently inundated areas, or in areas with prolonged inundation.
- sparse aquatic vegetation comprising relatively nutrient-poor permanently inundated areas and floodplain vegetation on previously dry floodplains, characterized by various species compositions, densities, and at various stages of development (W\_SAV)

Within the non-inundated areas, the following classes have to be considered:

- dry floodplains (D\_F)
- dry woodland and grassland of non-floodable areas (D\_WG)
- riparian woodland (D\_RW)
- bare soil (D\_BS)

Spectral reflectances of the classes mentioned above are shown in Fig 1. Most of the inundated (W) classes separate well from the non-inundated (D) classes, while there is an overlap between W\_DAV and D\_RW classes. Additionally, although (pure) classes W\_SAV and D\_F plot far apart, there is obviously a continuous transition between them.

Fires introduce additional complexity. Fire occurs in the area frequently, and the extent of burned patches can vary from several ha to thousands of km<sup>2</sup> [5]. Significantly, emergent aquatic vegetation such as papyrus or reeds does burn, even though it may be underlain by water. Fig. 2 presents spectral response in TM3 and TM6 of a part of the study area containing a fire scar. The morphology of the TM3/TM6 relationship is characteristic of surface temperature controlled by albedo and evaporation, as described for example in [9]. The line AB represents pixels where surface temperature is albedo-controlled. Surface temperature of pixels below this line is evaporation-controlled. Fire scars on dry land are characterized by high temperature (TM6) and low albedo (as approximated by TM3) and plot in the area marked “dry fire scars” in Fig. 2. Fire scars on inundated vegetation plot in the area marked “wet fire scars” in Fig.2.

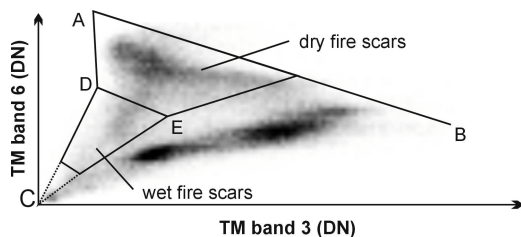


Figure 2 Reflectance characteristics (TM3 and TM6) of fire scars

#### 4. RESULTS

##### Comparison of accuracy of land/water discrimination using various methods

A comparison of the accuracy of land/water discrimination for the analysed methods is presented in Fig.3. In general, thresholding of the thermal band, and supervised classification give the best results with overall accuracy in order of 95%. Thresholding of the TM5/TM2 ratio and TC3 are less effective, with accuracy of 85%. The unsupervised classification gave accuracy in order of 95%. Such accuracies, although in

general high, are not considered satisfactory, given that we are dealing with only two classes. The performance of the methods is affected by the overlap of spectral characteristics of W\_DAV and D\_RW, as well as by arbitrariness of allocation of areas on the wet/dry floodplain boundary into either W\_SAV or D\_F.

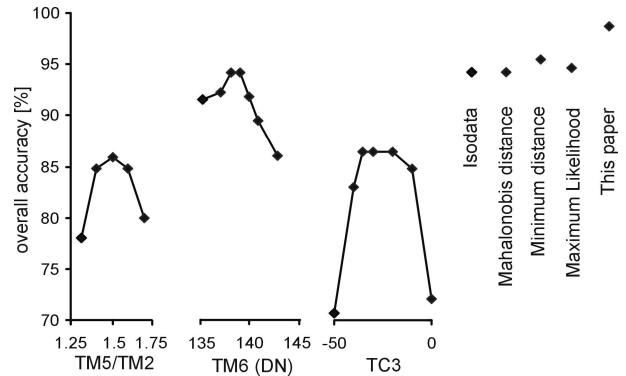


Figure 3 Comparison of accuracy of standard methods of land/water discrimination

The incorporation of such additional variables as NDVI and texture into unsupervised and supervised classification, did not improve results. We also attempted to incorporate contextual landscape information (neighbourhood, patch shape parameters etc.), but did not find contextual criteria that improved accuracy of the land/water discrimination. We have therefore devised a procedure for land/water discrimination that, in addition to spectral analyses, utilizes the fact that dryland vegetation that is confused with inundated vegetation in the spectral domain can be easily identified from texture in aerial photomosaics.

##### The Adopted Classification Method

The adopted classification method involves:

- 1) Determination, based on spectral characteristics only, of the extent of “inundated”, “dry” and “overlap” classes. This is done based on training areas of the two spectrally overlapping vegetation types, i.e. inundated dense vegetation, and riparian vegetation, and parallelepiped classification involving TM3, TM6, TM7 and the TM5/TM2 ratio.
- 2) Determination of the extent of fire scars within the inundated area. This is done based on the plot of TM3 vs. TM6. Pixels falling into the area marked in Fig. 2 as “wet fire scars” and defined by arbitrary defined points D and E are allocated to the “inundated” class.
- 3) Delineation of the extent of dry riparian vegetation falling within the “overlap” class from aerial photomosaics, and allocation of the respective pixels to “dry” class. This delineation is done manually based on interpretation of aerial photomosaics.

- 4) Classification as “dry” of all “overlap” polygons that are surrounded by “dry” class, and do not neighbour “inundated” polygons. This ensures that classification does not create discontinuous inundated patches, which agrees with observations in the field.
- 5) Unsupervised classification of the “overlap” class. This produces 3 subclasses with increasing reflectances in each of the bands. The two lower reflectance classes are allocated to the “inundated” class, and subsequent unsupervised classification of the third subclass is used to produce three more subclasses. The second-generation subclass with lowest reflectance is allocated to the “inundated” class.
- 6) Contextual allocation of polygons of the two of the remaining second-generation subclasses into “dry” or “inundated” based on the character and size of “dry” neighbourhood polygons and proximity to channels. Steps 5 and 6 ensure proper allocation of areas of the wet/dry floodplain boundary.

This procedure, when applied to the scene for which it was developed, gave an accuracy of 98% (Kappa=0.96). Verification of the procedure was done by applying it to an independent data set, i.e. an adjacent scene, with a set of 256 randomly distributed points for which inundation status was determined from the aerial photomosaic. The procedure achieved an accuracy of 98% (Kappa=0.95). Robustness of the procedure was checked by running it using three different sets of training areas of D\_RW and W\_DAV. Each of the inundation maps produced achieved the same accuracy as the original.

### Results of Land/Water discrimination procedure

Fig. 4 presents the annual flood frequency maps derived from the 14 coverages analysed. This map and other products such as time since last inundation will be used for locating sampling sites for biodiversity studies, vegetation dynamics studies and for analyses of change in the system.

### 5. SUMMARY AND CONCLUSIONS

Analysis of accuracy of traditional methods of land/water discrimination revealed that these are not straightforwardly applicable in the Okavango Delta, where dense aquatic vegetation and dense dryland vegetation can be easily confused in spectral domain. The method used here is based on training samples of vegetation-inundation classes that can easily be identified fromm. Improvement of accuracy compared to other methods is present, but more importantly, the procedure is robust and objective, and thus easily applicable to historic imagery, for which obtaining training areas for traditional classification, or determination of thresholds, is difficult or impossible.

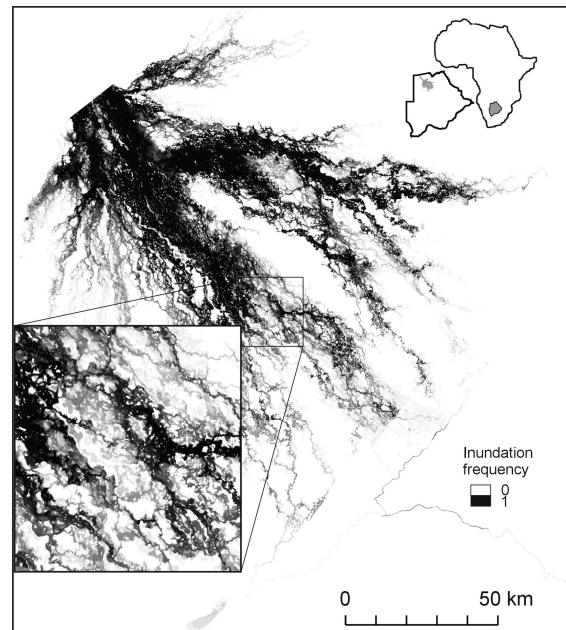


Figure 4 Inundation frequency (number of years inundated/number of analysed years) map

### 6. REFERENCES

1. Washington-Allen R. A., et al., A protocol for retrospective remote sensing-based ecological monitoring of rangelands, *Rangeland Ecology and Management*, Vol. 59, 19-29, 2006.
2. McCarthy J., et al., Flooding patterns in the Okavango Wetland in Botswana, between 1972 and 2000, *Ambio*, Vol. 7, 453-457, 2004.
3. McCarthy J., et al., Ecoregion classification in the Okavango Delta, Botswana from multitemporal remote sensing, *Int. J. Remote Sensing*, Vol. 26, 4339-4357, 2005.
4. Jellema A. et al., Preliminary vegetation map of the Okavango Delta. Water and Environmental Resources for Regional Development Project, <http://www.okavangochallenge.com>
5. Heidl M., *Fire and its effects on vegetation in the Okavango Delta, Botswana*, PhD thesis. Technical University Munich, Germany.
6. Bartsch A., ENVISAT ASAR global and wide swath mode capabilities for global monitoring of wetlands, this volume.
7. Milzow C., Role of remote sensing in hydrological modeling of the Okavango Delta, Botswana, this volume.
8. Ellery K. and Ellery W., *Plants of the Okavango Delta. A Field Guide*, Tsaro Publishers, Durban, South Africa, 1997.
9. Roerink G. J., et al., S-SEBI: A simple remote sensing algorithm to estimate the surface energy balance, *Physics and Chemistry of the Earth, Part B*, Vol. 25, 147-157, 2000.